

ARTICLE

Received 17 Oct 2014 | Accepted 5 May 2015 | Published 22 Jun 2015

DOI: 10.1038/ncomms8395

Peptidyl-prolyl isomerization targets rice Aux/IAAs for proteasomal degradation during auxin signalling

Hongwei Jing^{1,2,*}, Xiaolu Yang^{1,2,*}, Jian Zhang¹, Xuehui Liu³, Huakun Zheng^{1,2}, Guojun Dong⁴, Jinqiang Nian¹, Jian Feng¹, Bin Xia⁵, Qian Qian⁴, Jiayang Li¹ & Jianru Zuo¹

In plants, auxin signalling is initiated by the auxin-promoted interaction between the auxin receptor TIR1, an E3 ubiquitin ligase, and the Aux/IAA transcriptional repressors, which are subsequently degraded by the proteasome. Gain-of-function mutations in the highly conserved domain II of Aux/IAAs abolish the TIR1-Aux/IAA interaction and thus cause an auxin-resistant phenotype. Here we show that peptidyl-prolyl isomerization of rice OsIAA11 catalysed by LATERAL ROOTLESS2 (LRT2), a cyclophilin-type peptidyl-prolyl *cis/trans* isomerase, directly regulates the stability of OsIAA11. NMR spectroscopy reveals that LRT2 efficiently catalyses the *cis/trans* isomerization of OsIAA11. The *lrt2* mutation reduces OsTIR1-OsIAA11 interaction and consequently causes the accumulation of a higher level of OsIAA11 protein. Moreover, knockdown of the *OsIAA11* expression partially rescues the *lrt2* mutant phenotype in lateral root development. Together, these results illustrate cyclophilin-catalysed peptidyl-prolyl isomerization promotes Aux/IAA degradation, as a mechanism regulating auxin signalling.

chinaXiv:201605.01321v1

¹State Key Laboratory of Plant Genomics and National Center for Plant Gene Research, Institute of Genetics and Developmental Biology, Chinese Academy of Sciences, Beijing 100101, China. ²University of Chinese Academy of Sciences, Beijing 100049, China. ³Institute of Biophysics, Chinese Academy of Sciences, Beijing 100101, China. ⁴State Key Laboratory of Rice Biology, China National Rice Research Institute, Chinese Academy of Agricultural Sciences, Hangzhou 310006, China. ⁵College of Life Sciences, Peking University, Beijing 100871, China. *These authors contributed equally to this work. Correspondence and requests for materials should be addressed to J.Z. (email: jrzuo@genetics.ac.cn).

Auxin is an essential phytohormone that plays a fundamental role in the regulation of nearly all aspects of plant growth and development. In the past decades, extensive genetic and biochemical studies in *Arabidopsis* reveal that auxin signalling is mediated by a cascade that regulates the proteasomal degradation of the Auxin/INDOLE ACETIC ACID (Aux/IAA) transcriptional repressors in an auxin-dependent manner^{1–3}. When the intracellular concentration of auxin is low, Aux/IAs directly interact with AUXIN RESPONSE FACTORS (ARFs), a class of transcription factors that control the expression of downstream auxin-responsive genes, and thereby inhibit the transcriptional activity of ARFs. In response to specific developmental or environmental cues, auxin promotes the formation of a co-receptor complex consisting of a ubiquitin-ligase SCF^{TIR1/AFB} and Aux/IAs (refs 4–6). The auxin-dependent formation of the SCF^{TIR1}–Aux/IAA complex results in the ubiquitination of Aux/IAs, which are subsequently subjected to degradation through the 26S proteasomal degradation machinery. The proteasomal destruction of Aux/IAs relieves ARFs from the repressive complex and the active ARFs directly bind to the promoters to activate or repress the transcription of the downstream target genes^{7–11}.

The Aux/IAA repressor proteins contain four highly conserved domains, named domains I–IV (ref. 10). Of those domains, domain II, termed as the degron motif, is a key determinant of auxin-dependent degradation of Aux/IAs by mediating interaction with the auxin receptors TRANSPORT INHIBITOR RESPONSE1/AUXIN SIGNALING F-BOX PROTEINS (TIR1/AFBs). Genetic studies reveal that various gain-of-function mutations in domain II, largely located in the highly conserved central Gly–Trp–Pro–Pro–Val (GWPPV) motif, render Aux/IAs resistant to the auxin-induced proteasomal degradation, resulting in a dominant auxin insensitive phenotype^{7–10,12–14}. Notably, the auxin-dependent interaction between TIR1 and Aux/IAs is reduced or abolished by mutations in the GWPPV motif, illustrating the critical role of the domain II-mediated degradation of Aux/IAs in auxin signalling^{4,5,7,13,15}. Consistent with these observations, the analysis of the crystal structure of the *Arabidopsis* TIR1–auxin–IAA7 peptide complex reveals that the GWPPV motif of domain II is crucial for the formation of the co-receptor complex⁶. These studies demonstrate that the domain II-mediated degradation of Aux/IAs is a key step in auxin signalling. However, the possible involvement of post-translational modifications of Aux/IAs in regulating their stability remains elusive.

Recent studies suggest that rice, a model species of monocotyledonous plants, employs a regulatory mechanism of auxin signalling similar to that in *Arabidopsis*. Mutations in the rice LATERAL ROOTLESS2 (*LRT2*); also known as *Oryza sativa* CYCLOPHILIN2 or *OsCYP2* gene cause an auxin-resistant phenotype and defective development of lateral roots^{16,17}. *LRT2* encodes a putative cyclophilin-type peptidyl-prolyl *cis/trans* isomerase (PPIase) that catalyses the isomerization of peptide bonds at proline residues to specifically regulate protein conformational changes. The PPIase superfamily in higher eukaryotes includes cyclophilins (CYP), FK506-binding proteins, parvulins and PP2A phosphatase activators^{18,19}. In plants, cyclophilin-like genes have been identified from a variety of species, including both *Arabidopsis* and rice^{20–22}. A number of plant CYP genes, mainly in *Arabidopsis*, have been functionally characterized, involved in a variety of physiological and developmental processes, including in flowering, phytohormone signalling, stress responses and immune responses^{22–27}. Mutations in *LRT2*-like genes of the tomato *DIAGEOTROPICA* (*DGT*) and the moss *Physcomitrella patens* *PpDGT* genes also caused an auxin-resistant phenotype^{28–30}, indicating that this

class of highly conserved genes plays an important role in regulating auxin signalling in both lower and higher plants. However, how the cyclophilin-type PPIases function in auxin signalling remains unknown. Here we show that rice *LRT2*/*OsCYP2* acts as a functional cyclophilin to catalyse the peptidyl-prolyl *cis/trans* isomerization of the *OsAux/IAA* transcriptional repressors, thereby facilitating their binding to *OsTIR1* for subsequent proteasomal degradation and eventually activating auxin signalling.

Results

***LRT2* physically interacts with *OsAux/IAA* proteins.** Previous studies showed that mutations in the rice *LRT2*/*OsCYP2* gene (referred to as *LRT2* hereafter) cause an auxin-resistant phenotype and defective development of lateral roots^{16,17}. *LRT2* encodes a putative cyclophilin-type PPIase that catalyses the isomerization of peptide bonds at Pro residues. However, the specific substrates of *LRT2* remain unknown. We noticed that the *lrt2* mutant phenotype was similar to that of the rice *osiaa11*, *osiaa13* and *osiaa23* mutants^{31–33} (Supplementary Fig. 1). In particular, mutations in *LRT2*, *OsIAA11*, *OsIAA13* and *OsIAA23* all cause defective lateral root primordia, reduced tillering and plant height, and impaired panicle development, accompanying with the reduced expression level of auxin-inducible genes and the altered expression pattern of the *DR5:GUS* reporter gene^{16,17,31–33}, suggesting that *LRT2* may directly target *OsAux/IAA*s.

A close examination of the known mutations in domain II in various species revealed that these mutations occurred mainly in the two absolutely conserved Pro residues or, in a few cases, in the adjacent residues (Supplementary Fig. 2), suggesting that these two Pro residues play a critical role in regulating the stability of *Aux/IAA* proteins^{10,15}. If *LRT2* indeed targets *OsAux/IAA*s, these two types of proteins should directly interact. In a luciferase complementation imaging (LCI) assay, we found that *LRT2* interacted with all the tested *OsAux/IAA* proteins with various affinities when transiently expressed in tobacco leaves (Fig. 1a; Supplementary Fig. 3). Similarly, *LRT2* interacted with *OsIAA11* and *OsIAA13* in a yeast two-hybrid assay (Fig. 1b). A protein pull-down experiment revealed that *LRT2* directly interacted with *OsIAA11* and *OsIAA13* proteins (Fig. 1c). Moreover, *LRT2* interacted with *OsIAA11* and *OsIAA13* proteins *in planta* as revealed by a co-immunoprecipitation (Co-IP) assay (Fig. 1d; Supplementary Fig. 4). In the Co-IP experiment, we reproducibly observed an extra band with the reduced size in the *osiaa11* sample by using two batches of antibodies generated from different mice. We speculate that this band may be a degraded product of *osiaa11* mutant protein in the assay. Notably, the *osiaa11* (*OsIAA11*^{P106L}) gain-of-function mutant protein showed the reduced interaction with *LRT2* compared with its wild-type partners (Fig. 1d). When transiently expressed in tobacco leaves, the direct interactions between *LRT2* and *OsIAA11* or *OsIAA13* were also detected by a Co-IP assay (Supplementary Fig. 5). Moreover, mutations in the conserved Pro residues (*OsIAA11*^{P105L} and *OsIAA13*^{P91L}) also caused the reduced interactions with *LRT2*, suggestive of the importance of these Pro residues in mediating the *LRT2*–*OsAux/IAA* interaction. Taken together, these results demonstrated that *LRT2* directly interacts with *OsIAA11* and *OsIAA13* and the interaction is regulated by domain II of *OsAux/IAA* proteins.

LRT2 catalyses *cis/trans* isomerization of *OsIAA11* peptide.

Given that *LRT2* physically interacts with *OsIAA11* and *OsIAA13*, we next explored whether *LRT2* is capable of catalysing the peptidyl-prolyl isomerization of *OsAux/IAA* proteins by

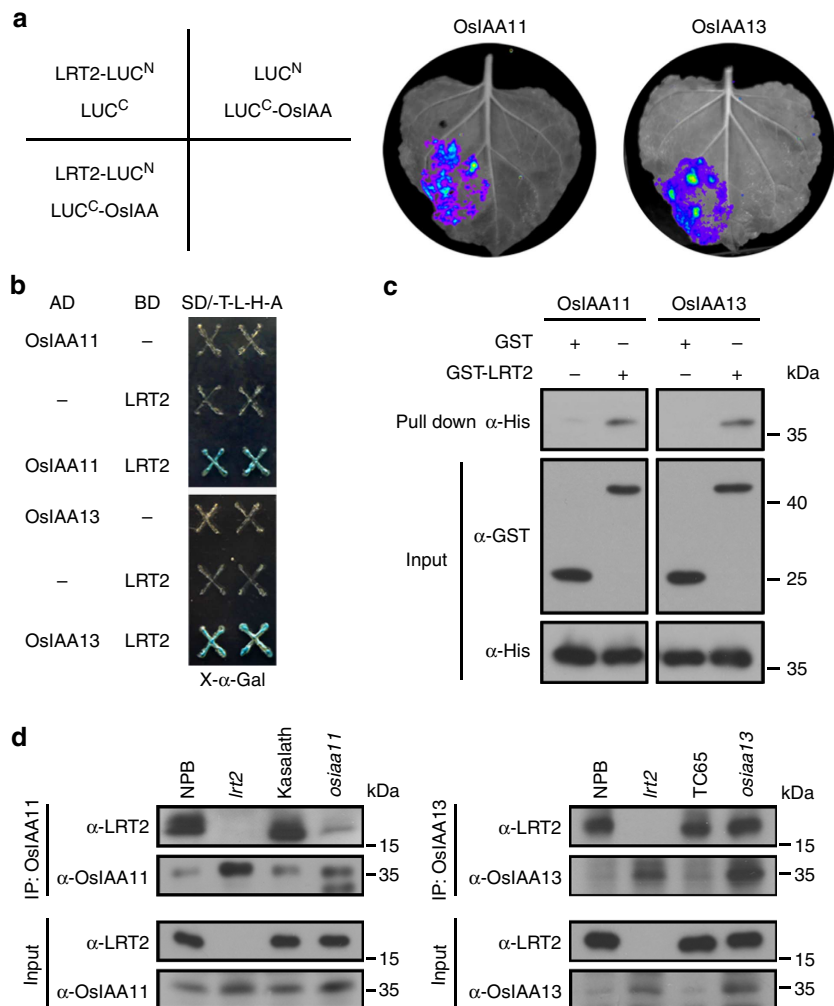


Figure 1 | LRT2 interacts with OsIAA proteins. (a) Analysis of the interaction of LRT2 with OsIAA11 and OsIAA13 transiently expressed in tobacco leaves by the luciferase complementation imaging assay. (b) Analysis of the interaction of LRT2 with OsIAA11 and OsIAA13 by the yeast two-hybrid assay. (c) GST-LRT2 directly interacts with His-OsIAA11 (OsIAA11) and His-OsIAA13 (OsIAA13) as analysed by the pull-down experiment. GST protein is served as a negative control. (d) Co-immunoprecipitation analysis of the interaction of LRT2 with OsIAA11 and OsIAA13 in wild-type (Nipponbare or NPB, Kasalath and Taichung 65 or TC65), *lrt2*, *osiaa11* and *osiaa13* seedlings.

NMR spectroscopy. To this end, we examined the capability of LRT2 for catalysing *cis/trans* conformational exchange of a peptide of 12 residues derived from domain II of OsIAA11 (residues 98–109), which differed in one residue with OsIAA13 and *Arabidopsis* IAA7 in this region (Fig. 2a; Supplementary Fig. 2). Analysis of the crystal structure of the TIR1-IAA7 co-receptor revealed that Trp⁸⁶ and Pro⁸⁸ in the conserved central GWPPV motif of the IAA7 peptide are inserted in the auxin-binding pocket of TIR1 and stacking against the auxin indole ring and the auxin side chain, respectively, whereas Pro⁸⁷ in *cis*-conformation is important for maintaining the binding conformation⁶.

We found that LRT2 efficiently catalysed *cis/trans* conformational exchanges of the OsIAA11 peptide as evident by the detection of exchange peaks resulting from proline isomerization in the ROESY (rotating frame Overhauser effect spectroscopy) spectra, whereas no exchange peak was detected in the absence of LRT2 (Fig. 2b,c), suggesting that LRT2 is capable of catalysing conformational exchanges of the OsIAA11 peptide. We also analysed the PPIase activity of LRT2^{G72A} mutant protein. Gly⁷² is a highly conserved residue located in the PPIase domain (Supplementary Fig. 6a) and mutations in this residue of rice *LRT2/OsCYP2* and moss *PpDGT* cause severely impaired auxin

signalling^{17,30}. Homologous structure modelling based on the crystal structure of wheat (*Triticum aestivum*) TaCypA-1 (PDB code: 4E1Q)³⁴, a cyclophilin sharing 87% identity with LRT2, revealed that Gly⁷² is located at the surface of LRT2 immediately adjacent to a β -sheet (Supplementary Fig. 6b). LRT2^{G72A}/cyp2-2 recombinant protein, which was less stable than wild-type LRT2 recombinant protein (Supplementary Fig. 7a), showed markedly decreased PPIase activity in catalysing the *cis/trans* isomerization of the OsIAA11 peptide (Fig. 2b,c; Supplementary Fig. 6c,d). LRT2^{G72A}/cyp2-2 mutant protein was undetectable in the *cyp2-2* mutant¹⁷ (Supplementary Fig. 7b). Similarly, when transiently expressed in tobacco leaves, no LRT2^{G72A}/cyp2-2 mutant protein was detected (Supplementary Fig. 7c). These results indicate that Gly⁷² of LRT2 is important for both its stability and the enzymatic activity.

For the two tandem proline residues specific to the conformation of the Trp¹⁰⁴-Pro¹⁰⁵ and Pro¹⁰⁵-Pro¹⁰⁶ motifs, four conformers in the solution were predicted³⁵, namely T¹⁰⁵T¹⁰⁶, T¹⁰⁵C¹⁰⁶, C¹⁰⁵T¹⁰⁶ and C¹⁰⁵C¹⁰⁶, where T and C represented *trans* and *cis* conformation, respectively. In the OsIAA11 peptide, the signals of the minor conformers are nearly invisible with serious signal overlapping. Although we observed some exchange

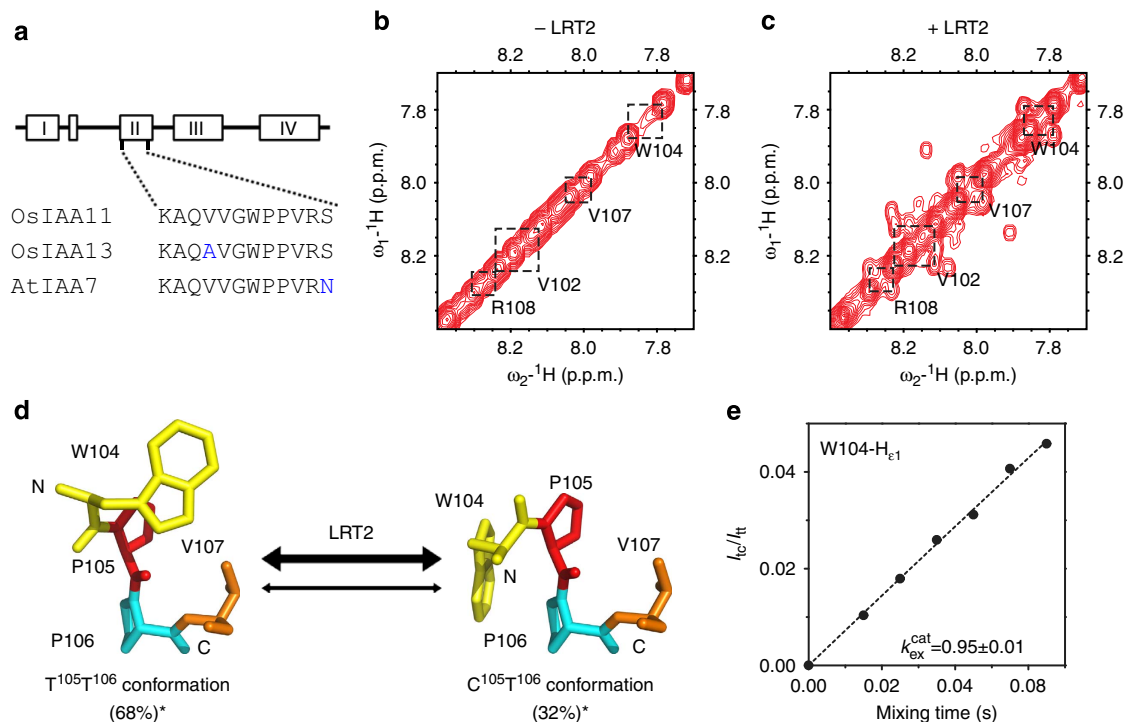
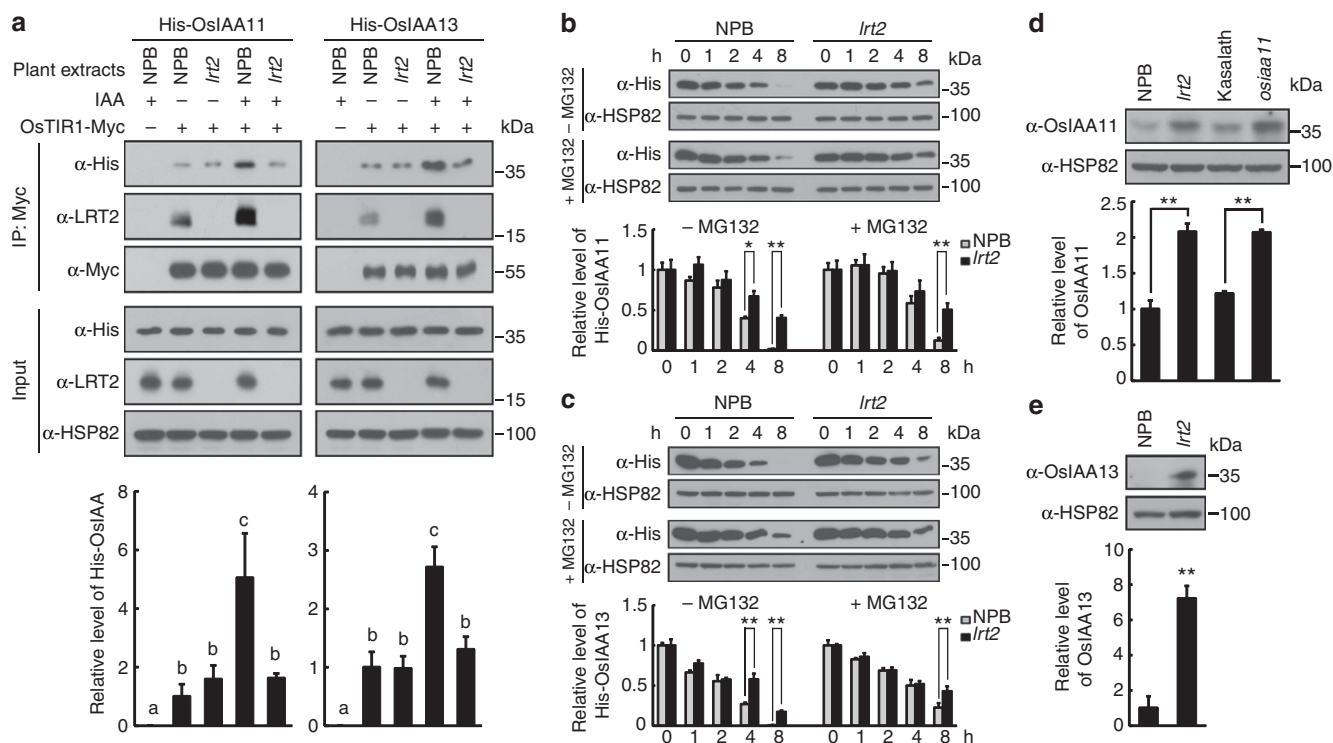


Figure 2 | LTR2 catalyses isomerization of OsIAA11 peptide. (a) Top: the structural features of Aux/IAA proteins. Domains I through IV are highlighted as boxes. Bottom: the alignment of partial sequences in domain II of rice and *Arabidopsis* Aux/IAs. Amino-acid residues in OsIAA13 and AtIAA7 that differed with those of OsIAA11 are highlighted in blue. (b,c) Selected region of the 110 ms mixing time ROESY spectra of the OsIAA11 peptide in the absence (b) and the presence (c) of LRT2 recombinant protein. Signals from the major conformers of residues V102, W104, V107 and R108 are labelled at the positions where exchange cross peaks are expected. (d) Approximate two-state exchange process of the OsIAA11 peptide. The exchange rate is indicated by the thickness of the double-arrow lines. * indicates the mix populations of the $T^{105}T^{106} + T^{105}C^{106}$ and $C^{105}T^{106} + C^{105}C^{106}$ obtained from the integration of the $H_{\epsilon 1}$ signals of W104 in the 1D 1H spectrum, respectively, with $T^{105}T^{106}$ and $C^{105}T^{106}$ as major conformers. (e) Dependence of cross/diagonal peak intensity ratios on ROE mixing time in the presence of LRT2 for $H_{\epsilon 1}$ of residue W104 of the OsIAA11 peptide. Intensities of diagonal peaks with *trans* and *cis* conformations are labelled as I_t and I_{ct} , respectively. The intensities of exchange peaks resulting from the LRT2-catalysed *trans*-to-*cis* and *cis*-to-*trans* isomerization are labelled as I_{tc} and I_{ct} , respectively. Catalysed exchange rate constant k_{ex}^{cat} was derived from data points fitted to equation (2) in Methods.

peaks from the minor conformers in the ROESY spectra (Supplementary Fig. 8), it is technically impossible for the signal assignment and difficult to calculate the rate constants of the minor conformers. Considering the lowest *cis* population of Xaa-Pro bond, where Xaa as a proline³⁵ and the type II helix with *trans* conformation dominating the poly-Pro sequence, the two major conformers of OsIAA11 peptide were deduced as $T^{105}T^{106}$ and $C^{105}T^{106}$, while the minor conformers were predicted as $T^{105}C^{106}$ and $C^{105}C^{106}$ (Fig. 2d). Since most of Pro¹⁰⁵-Pro¹⁰⁶ amide bonds adopt *trans* conformation, the complex four-state exchange equilibrium could be well approximated by a two-state equilibrium and the exchange rate constant could then be estimated by curve fitting (Fig. 2e). In the presence of LRT2, the peptidyl-prolyl *cis/trans* conformational exchange was significantly accelerated with $k_{ex}^{cat} = 0.95 \pm 0.01 \text{ s}^{-1}$ (Fig. 2e), substantially faster than the uncatalysed isomerization rate, which is typically $< 0.01 \text{ s}^{-1}$ (refs 36,37). Taken together, these results demonstrate that LRT2 specifically catalyses the *cis/trans* isomerization of the OsIAA11 peptide.

LRT2 negatively regulates the stability of OsIAA11. Consistent with the above results, the *Arabidopsis* IAA7 peptide, which shows nearly identical sequence as the OsIAA11 peptide (Fig. 2a), presents as the $C^{87}T^{88}$ (equivalent to $C^{105}T^{106}$ of OsIAA11) conformer in the crystal structure of the TIR1-IAA7 co-receptor⁶. Moreover, the *Arabidopsis* domain II mutant proteins *iaa3/shy2*, *iaa7/axr2-1* and *iaa17/axr3-1*, which carry mutations in

the highly conserved proline residues (see Supplementary Fig. 2), are incapable of binding the TIR1 receptor^{4,5,7,13,15}. These observations, together with the results presented in Figs 1 and 2, raise the possibility that LRT2-catalysed *cis/trans* isomerization of OsAux/IAs is critical for the formation of a functional OsTIR1-OsIAA co-receptor. To test this hypothesis, we examined the possible regulatory role of LRT2 on the OsTIR1-OsIAA11 interaction by a Co-IP experiment. OsTIR1-Myc protein transiently expressed in tobacco leaves and purified by immunoprecipitation was incubated with His-OsIAA11 recombinant protein and extracts prepared from wild-type or *lrt2* plants, and the OsTIR1-OsIAA11 interaction was examined by a Co-IP experiment. In the absence of auxin, OsTIR1-Myc interacted with His-OsIAA11 in a similar affinity when incubated with extracts prepared from wild-type or *lrt2* plants (Fig. 3a), a result similar to that previously observed in *Arabidopsis*^{15,38}. This result may be attributed to the presence of a significant portion of the $C^{105}T^{106}$ conformer in the absence of LRT2 (see Fig. 2). The interaction between OsTIR1-Myc and His-OsIAA11 or His-OsIAA13 was substantially enhanced by auxin when incubated with extracts prepared from wild-type plants. However, when incubated with extracts prepared from *lrt2* plants, the interaction between OsTIR1-Myc and His-OsIAA11 or His-OsIAA13 was not responsive to auxin (Fig. 3a), indicating that the LRT2 activity is required for the auxin-dependent OsTIR1-OsIAA interaction. Notably, neither the LRT2 messenger RNA (mRNA) level nor the accumulation of LRT2 protein was regulated by auxin (Supplementary Fig. 9). However, LRT2 protein, which was in a



same protein complex with OsTIR1 and OsIAA11, was enriched in the complex when treated with auxin (Fig. 3a), implying that the binding of LRT2 to the OsTIR1–OsIAA11 co-receptor is positively regulated by auxin.

To explore the functional significance of the OsTIR1–OsIAA–LRT2 complex, we next performed an *in vitro* degradation assay to examine the stability of OsIAA11 and OsIAA13. When incubated with the protein extracts prepared from wild-type or *lrt2* plants, both His–OsIAA11 and His–OsIAA13 recombinant proteins showed the reduced degradation in the absence of LRT2 and the reduced response to MG132, a specific inhibitor of the proteasomal degradation pathway (Fig. 3b,c). Moreover, the accumulation of OsIAA11 and OsIAA13 proteins was increased in *lrt2* plants compared with wild type (Fig. 3d,e). These results indicate that the LRT2-catalysed *cis/trans* isomerization of OsAux/IAA proteins is critical for the formation of the OsTIR1–OsIAA co-receptor, thereby for the proteasomal degradation of the transcriptional repressors.

OsIAA11 genetically acts downstream of LRT2. Data presented above indicate that LRT2 negatively regulates the accumulation of the auxin signalling repressor OsAux/IAAs. We then reasoned that the reduced expression of the *OsAux/IAA* genes might partially relieve the *lrt2* mutant phenotype. To this end, we

generated transgenic rice plants knocking down the expression of *OsIAA11* by RNA interference (RNAi). The steady level of *OsIAA11* mRNA in the transgenic plants was decreased $\sim 80\%$ compared with that of wild type (Fig. 4a). Other examined *OsAux/IAA* genes were expressed at various levels. Compared with wild-type plants, the expression of *OsIAA22* and *OsIAA31* was reduced $\sim 50\%$, whereas the expression of *OsIAA14*, *OsIAA16*, *OsIAA20* and *OsIAA30* was also decreased in the transgenic lines (Supplementary Fig. 10). The target region of *OsIAA11* (218 bp) showed the highest homology with *OsIAA1* (95.1%), *OsIAA30* (92.3%), *OsIAA14* (92.1%), *OsIAA31* (90.9%) and *OsIAA15* (87.0%), which did not correlate with the expression levels of these genes in the RNAi-transgenic lines. While the cause of the reduced expression of other non-target *OsIAA* genes in the RNAi-transgenic plants remains unknown, the expression of *OsIAA11* was downregulated to a significantly greater degree compared with wild-type plants (Fig. 4a; Supplementary Fig. 10). Consistently, the accumulation of OsIAA11 protein was also reduced in the RNAi-transgenic lines in the *lrt2* mutant background (Fig. 4b). Note that the reduction of the OsIAA11 protein level was less marked than that of *OsIAA11* mRNA level in the RNAi-transgenic plants (Fig. 4a,b), which might result from the increased stability of OsIAA11 protein in the *lrt2* mutant background.

The *lrt2* mutation caused the markedly reduced number of lateral roots compared with that of wild type^{16,17} (Fig. 4c,d).

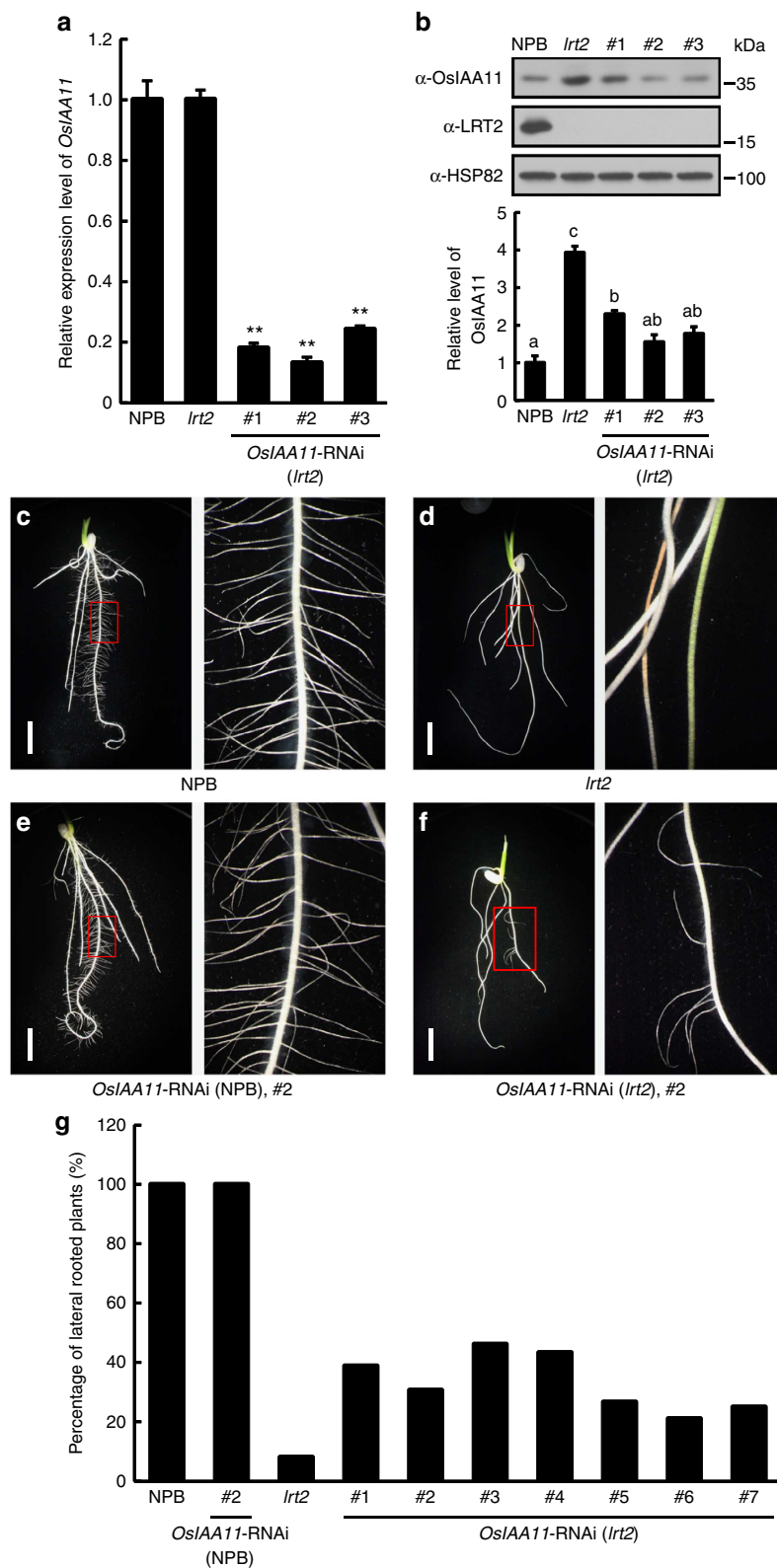


Figure 4 | Knocking down the *OsIAA11* expression partially rescues the *lrt2* mutant phenotype. (a) Analysis of the expression level of *OsIAA11* in RNAi-transgenic seedlings (line numbers are given below the graph) by qRT-PCR. Error bars indicate s.d.; ** $P < 0.01$ (Student's *t*-test). (b) Immunoblotting analysis of the accumulation of *OsIAA11* protein in RNAi-transgenic seedlings (line numbers are given below the graph). Equal loading is verified by the analysis of HSP82 protein. Quantitative analysis of the relative level of *OsIAA11* protein is presented below the blots. Error bars indicate s.d.; different letters indicate $P < 0.05$ (LSD multiple range tests). (c-f) The root phenotype of 10-day-old seedlings with the indicated genotypes. In each panel, the right side shows the enlarged view of the boxed region at the left side. Scale bars, 1 cm. (g) Quantitative analysis of the percentage of lateral rooted plants in 10-day-old seedlings with the indicated genotypes ($n \geq 30$ for each genotype). Note that, knocking down the *OsIAA11* expression in the wild-type background has no detectable effect on lateral root development.

The knockdown of the *OsIAA11* expression in *lrt2* partially rescued defective development of lateral roots and the primary roots (Fig. 4e,f; Supplementary Fig. 11). In the RNAi-transgenic plants, the frequency of producing lateral roots was substantially higher than that of *lrt2* (Fig. 4g). These results demonstrate that *LRT2* genetically acts upstream of *OsIAA11* to positively regulate lateral root development.

Discussion

It has long been known that auxin signalling is activated via a derepression mechanism, in which auxin induces the proteasomal degradation of the signalling repressor Aux/IAAs^{9,10}. Yet, it remains uncertain if post-translational modifications are involved in the regulation of the stability of Aux/IAAs^{15,38}. We have presented genetic and biochemical evidence demonstrating that the rice cyclophilin *LRT2/CYP2* catalyses the peptidyl-prolyl *cis/trans* isomerization of the OsAux/IAA transcriptional repressors, leading to their binding to OsTIR1 for the targeted proteasomal degradation and eventually activating auxin signalling (Fig. 5).

Considering that the key components, including *LRT2*-like proteins and Aux/IAAs, are highly conserved in both lower and higher plants and that the loss-of-function mutations in tomato *DGT* and moss *PpDGT* cause a similar auxin-insensitive phenotype^{29,30}, the cyclophilin-catalysed isomerization of the Aux/IAA transcriptional repressors may represent a general mechanism in regulating auxin signalling in the plant kingdom. In agreement with this notion, *LRT2/OsCYP2* was found to directly interact with *OsSGT1* (suppressor of G2 allele of *skp1*)¹⁷,

whose *Arabidopsis* homologous gene *AtSGT1b* was identified from a genetic screen for the enhancers of *tir1-1* and was characterized as co-chaperone to be required for the SCF^{TIR1}-mediated degradation of Aux/IAA proteins³⁹. Moreover, mutations in the *Arabidopsis* *SIR1* gene, which encodes a protein sharing homology with peptidyl-prolyl isomerase, cause an auxin hypersensitive phenotype, thus providing an additional line of genetic evidence supporting a regulatory role of conformational changes on Aux/IAA proteins⁴⁰. Evidence presented in this study demonstrates that *LRT2* modulates the *cis/trans* isomerization exchanges of *OsIAA11* and, possibly, *OsIAA13*. Two lines of evidence suggest that *LRT2* may also target other OsAux/IAA proteins. First, *LRT2* interacts with all the tested OsAux/IAA proteins in the luciferase complementation assay, suggesting that these OsAux/IAA proteins are potential targets of *LRT2*. Second, the knockdown of the *OsIAA11* expression only partially rescues the *lrt2* mutant phenotype, implying that other downstream factors are likely involved in the *LRT2*-mediated auxin signalling. In this regard, *LRT2* protein may regulate a larger repertoire of OsAux/IAA transcriptional repressors.

CYP have been found to be involved in the signalling of several phytohormones, including auxin, brassinosteroid, gibberellic acid (GA) and jasmonic acid^{16,17,23–25,41–43}. Among these and other phytohormones, the activation of the signalling pathways of GA, jasmonic acid and strigolactone also utilize a derepression mechanism by the proteasomal degradation of specific repressors in a manner similar to that of auxin^{44–48}. Interestingly, a GA-insensitive dwarf (*gaid*) mutant of wheat was characterized to be insensitive to exogenous GA, correlated to the elevated levels of the GA signalling repressor Rht/DELLA protein and a putative cyclophilin TaCYP20-2 protein. Moreover, the overexpression of *TaCYP20-2* causes the accumulation of excessive amount of Rht/DELLA repressor protein and a dwarf phenotype similar to that of the *gaid* mutant, suggesting that the putative cyclophilin TaCYP20-2 is involved in DELLA protein degradation during GA signalling⁴². Therefore, the cyclophilin-mediated peptidyl-prolyl *cis/trans* isomerization is not only required for binding of the OsAux/IAAs repressors to OsTIR1 but may also play an important role in regulating other phytohormone signalling pathways.

In summary, we have defined a regulatory role of the rice cyclophilin *LRT2* in auxin signalling by mediating the *cis/trans* isomerization of the Aux/IAA transcriptional repressors, thereby facilitating their proteasomal degradation. Whereas our discovery has revealed a new layer of the regulatory scheme in auxin signalling, the precise molecular mechanism of the auxin-promoted *LRT2* activity remains challenging for future studies.

Methods

Plant materials and growth conditions. Wild-type rice of Nipponbare, Taichung 65 (*Oryza sativa* L. ssp. *japonica*), and Kasalath (*Oryza sativa* L. ssp. *indica*) were used in this study. The *lrt2* mutant is in the Nipponbare background and has been previously described^{16,49}. The *cyp2-2* and *osiaa11* mutants are in the Kasalath background and the *osiaa13* mutant is in the Taichung 65 background^{17,31,32}, which were kindly provided by Dr Xiaorong Mo, Dr Ping Wu and Dr Yoshiaki Inukai, respectively.

Rice plants were grown in the fields in Beijing, Hangzhou and Hainan with routine management. To analyse the seedling phenotype under the tissue culture condition, seeds were surface sterilized with 75% ethanol for 5 min, then sterilized with 30% bleach for 30 min and rinsed six times with sterile water. Sterilized seeds were plated on MS medium (1/2 MS salts, 1% sucrose, 0.8% agar, pH 5.9) and grown under 28 °C at a photoperiod of 16-h light/8-h dark in a greenhouse.

Genetic transformation of rice was performed as described⁵⁰. In brief, calli derived from rice embryos were infected with agrobacteria cells carrying a target expression vector for 1–2 min. The infected calli were cultured on N6-AS medium (3.981 g l⁻¹ N6 salts, 2 mg l⁻¹ 2,4-D, 0.3 g l⁻¹ casein hydrolysate, 30 g l⁻¹ sucrose, 10 g l⁻¹ glucose, 15 mg l⁻¹ acetosyringone, 4 g l⁻¹ phytigel, pH 5.2) for 3 days at 25 °C. After washing with sterile water containing 500 mg l⁻¹ carbenicillin for

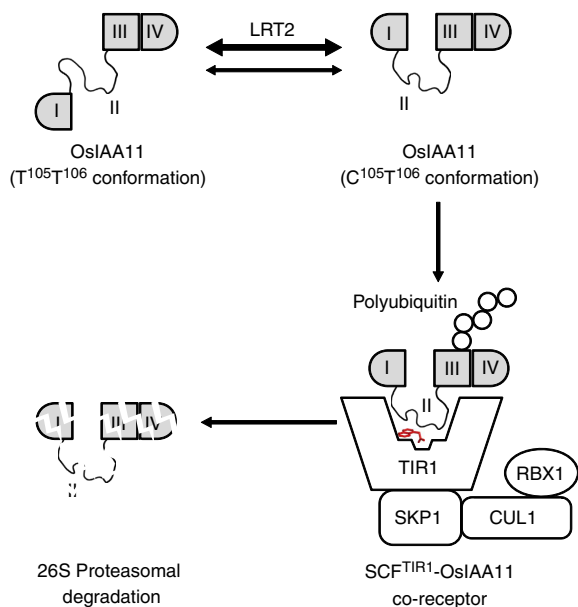


Figure 5 | A proposed model for the *LRT2*-regulated auxin signalling. The *OsIAA11* transcriptional repressor is present as two exchangeable major conformers $T^{105}T^{106}$ and $C^{105}T^{106}$ (indicated by a thin double-headed line). The cyclophilin *LRT2* catalyses the peptidyl-prolyl *cis/trans* isomerization at the Trp^{104} - Pro^{105} peptide bond of *OsIAA11*, accelerating the formation of the Pro^{105} -*cis* conformer (indicated by a thick double-headed line). In the presence of auxin (red molecule), $C^{105}T^{106}$ conformers interact with the SCF^{TIR1} complex with a higher affinity than $T^{105}T^{106}$ conformers. The formation of the SCF^{TIR1}-*OsIAA11* co-receptor facilitates the ubiquitination and subsequent proteasomal degradation of *OsIAA11*, which consequently leads to the two-state equilibrium shifting in favour of the formation of $C^{105}T^{106}$ conformers. Domains I through IV are indicated in the *OsIAA11* molecule.

three times, the calli were cultured on selection medium (3.981 g l⁻¹ N6 salts, 2 mg l⁻¹ 2,4-D, 0.5 g l⁻¹ casein hydrolysate, 0.5 g l⁻¹ L-proline, 30 g l⁻¹ sucrose, 4 g l⁻¹ phytigel, 200 mg l⁻¹ carbenicillin, 200 mg l⁻¹ cefotaxime, 50 mg l⁻¹ hygromycin B, pH 5.8) for 2 weeks and the putative positive calli were transferred onto fresh selection medium for an additional 2 weeks. Hygromycin B-resistant calli were then transferred onto differentiation medium (4.4 g l⁻¹ MS salts, 30 g l⁻¹ sucrose, 30 g l⁻¹ sorbitol, 2 g l⁻¹ casein hydrolysate, 0.02 mg l⁻¹ NAA, 2 mg l⁻¹ kinetin, 4 g l⁻¹ phytigel, 50 mg l⁻¹ carbenicillin, 50 mg l⁻¹ hygromycin B, pH 5.8) and cultured for several weeks to regenerate seedlings or plantlets. The regenerated seedlings were then transferred onto rooting medium (2.2 g l⁻¹ MS salts, 0.5 g l⁻¹ L-proline, 0.5 g l⁻¹ casein hydrolysate, 30 g l⁻¹ sucrose, 0.5 mg l⁻¹ IBA, 4 g l⁻¹ phytigel, pH 5.8) and cultured for several weeks.

Plasmid construction. The coding sequences of *OsIAA11* and *OsIAA13* were PCR amplified from rice complementary DNA (cDNA) and the stop codons were eliminated during PCR. The PCR fragments were cloned into the *Bam*HI and *Sal*I sites of pGEX4T-1 (Amersham Biosciences) and pET28a (Novagen) to generate pGST-OsIAA and pHis-OsIAA expression vectors, respectively. The pGST-LRT2 and pHis-LRT2 constructs were generated in a similar way using the *Eco*RI and *Sal*I sites.

To create the pGADT7-OsIAA constructs, the coding sequences of *OsIAA11* and *OsIAA13* were PCR amplified from rice cDNA and the stop codons were eliminated. The PCR fragments were cloned into the *Eco*RI and *Sal*I sites of pGADT7 (Clontech). The pGBKT7-LRT2 construct was generated in a similar way.

The coding sequence of *LRT2* was PCR amplified from rice cDNA and the stop codons were eliminated. The gene was inserted in the *Kpn*I and *Sal*I sites of pCAMBIA-nLUC⁵¹. The coding sequences of *OsIAA1*, *OsIAA11*, *OsIAA13*, *OsIAA20*, *OsIAA22*, *OsIAA23* and *OsIAA30* were PCR amplified from rice cDNA and the stop codons were eliminated. The *OsIAA20* and *OsIAA30* genes were cloned into the *Kpn*I and *Pst*I sites, and the others were cloned into the *Kpn*I and *Sal*I sites of pCAMBIA-cLUC⁵¹.

The *OsIAA11*-RNAi (*OsIAA11*-RNAi) vector was constructed by sequentially inserting two inverted copies of a 218-base pair (bp) cDNA fragment of *OsIAA11* (nucleotides 143–361; the first nucleotide of the putative translation codon was referred to as +1) into the pTCK303 vector⁵² using the *Bam*HI/*Kpn*I and *Spe*I/*Sac*I sites, respectively.

The pWMI101 vector⁵³ was used to construct 35S::*OsIAA11*-FLAG, 35S::*OsIAA13*-FLAG and 35S::*LRT2*-Myc expression vectors. The coding sequences of *OsIAA11*, *OsIAA13* and *LRT2* were PCR amplified from rice cDNA and the stop codons were eliminated. The fragments were cloned into the *Kpn*I and *Xma*I sites of pBluescript SK (Stratagene), in-frame fused to a FLAG tag or 6 × Myc tag to generate fusion genes, which were cloned into the *Kpn*I/*Xba*I sites of pWMI101 vector.

To construct 35S::*OsTIR1*-Myc-NOS vector, the 35S promoter fragment, a 6 × Myc tag and the NOS terminator sequences were ligated into the binary vector pCAMBIA1300 using *Eco*RI/*Sac*I, *Sal*I/*Pst*I and *Pst*I/*Hind*III sites, respectively. The coding sequence of *OsTIR1* (lacking the stop codon) was inserted into the pCAMBIA1300-35S-Myc-NOS vector using the *Bam*HI and *Sal*I sites.

Site-directed mutagenesis was performed using the Easy Mutagenesis System (TransGen Biotech, Beijing) according to the manufacturer's instructions.

All the binary expression vectors were introduced into *Agrobacterium tumefaciens* strain EHA105 and then used for the transformation of rice or the infiltration of tobacco leaves. All primers used for plasmid construction are listed in Supplementary Table 1. The accession numbers of all genes analyzed in this study are listed in Supplementary Table 2.

Quantitative reverse transcription-PCR. Total RNA was prepared using the RNeasy Pure Plant RNA Purification Kit (Qiagen Biotech). Quantitative reverse transcription-PCR (qRT-PCR) was performed using the UltraSYBR Mixture (CWBio) according to the manufacturer's instructions. The reactions were run in a CFX96 REAL-Time PCR Detection System (Bio-Rad). The relative expression level of the target genes was analysed with the delta-delta Ct method and normalized to the expression level of *OsACTIN2*. All of the experiments were repeated for at least twice (two biological repeats with three technical repeats for each experiment). The primers used for qRT-PCR are listed in Supplementary Table 1.

Antibody preparation and immunoblotting. The anti-LRT2 polyclonal antibody has been previously described¹⁶. To prepare anti-*OsIAA11* and anti-*OsIAA13* antibodies, the full-length cDNA fragments were used to produce recombinant proteins tagged with 6 × His. The purified 6 × His-tagged recombinant proteins were used to immunize mice and rabbits, respectively. Immunoblotting was performed as described previously⁵⁴. Total cellular proteins were prepared by grinding plant materials in liquid nitrogen and then extracted in grinding buffer (50 mM Tris-HCl, pH 8.0, 150 mM NaCl, 1% Nonidet P-40, 0.5% sodium deoxycholate, 0.1% SDS and 1 mM phenylmethylsulfonyl fluoride). After centrifugation twice at 14,000g for 15 min at 4 °C, the supernatant was collected and then subjected to SDS-polyacrylamide gel electrophoresis. After the run, proteins were electrically transferred onto a polyvinylidene difluoride membrane,

and then detected with a primary antibody of indicated (usually at 1:5,000 dilution). The blot was incubated with a secondary antibody (horseradish peroxidase-conjugated goat anti-rabbit IgG or horseradish peroxidase-conjugated goat anti-mouse IgG; Beijing Dingguo Changsheng Biotechnology) at 1:50,000 dilution. The signal was detected using a SuperSignal Western Femto Maximum Sensitivity Substrate kit (Thermo Scientific, Cat no.: 34096) according to the manufacturer's instructions. Rice HSP82 was used as a loading control. In most immunoblotting experiments, the blot was first probed with an antibody specific to a target protein and then stripped, followed by re-probing the blot with anti-HSP82 antibody. Occasionally, two technical replicates (gels) were simultaneously performed and then analysed with antibodies against the specific targets and HSP82, respectively (Fig. 3d). The target bands and loading control bands were quantified using NIH ImageJ (version 1.42q, <http://rsbweb.nih.gov/ij/>) and the mean values of 3–5 independent experiments were presented with statistical analysis (LSD multiple range tests for Fig. 3a and Fig. 4b; Student's *t*-test for all other experiments) of significant differences when applicable. Uncropped versions of all blots are presented in Supplementary Figures 12–14.

Yeast two-hybrid assay. The coding sequences of *OsIAA11* and *OsIAA13* were cloned into the prey vector pGADT7 (Clontech). The *LRT2* full-length coding sequence was cloned into the bait vector pGBKT7 (Clontech). The bait and prey constructs were co-transformed into the yeast (*Saccharomyces cerevisiae*) strain AH109 (Clontech). The transformants were grown on SD-Leu/-Trp plates for 3–5 days at 30 °C. The interactions between bait and prey were examined on the control media-LT (SD-Leu/-Trp) and selective media-LTHA (SD-Leu/-Trp/-His/-Ade) supplemented with X-α-gal by incubating the plates at 30 °C for 3–5 days.

LCI assay. The detection of protein-protein interactions by the LCI assay was performed as described⁵¹. *LRT2* and *OsIAA* cDNA fragments were in-frame fused with *nLUC* and *cLUC* in the pCAMBIA-nLUC and pCAMBIA-cLUC vectors⁵¹, respectively. The resulting binary expression vectors were transformed into *Agrobacterium* strain EHA105. *Agrobacterium* cells carrying various expression vectors were co-infiltrated into *Nicotiana benthamiana* (*N. benthamiana*) leaves with appropriate controls. After the infiltration, plants were placed at 22 °C for 72 h and the fluorescent images were collected with a low-light cooled charge-coupled device (CCD) imaging apparatus (Andor iXon). The experiment was repeated three times with independent biological replicates.

Pull-down assay. Protein pull-down assay was performed as described⁵⁵ with minor modifications. In brief, purified GST, GST-LRT2, His-OsIAA11 and His-OsIAA13 proteins were immobilized on GST beads (Glutathione Sepharose 4B; GE Healthcare). Immobilized Sepharose beads containing 2 μg GST or GST-LRT2 fusion proteins were mixed with 2 μg His-tagged proteins and then incubated at 4 °C for 2 h. The beads were collected by centrifugation and then washed six times with washing buffer (10 mM phosphate buffer saline, pH 7.4, 150 mM NaCl, 0.2% Triton X-100 and 1 mM phenylmethanesulfonyl fluoride) at 4 °C. The beads were resuspended in SDS-polyacrylamide gel electrophoresis sample buffer and then analysed by immunoblotting.

In vitro turnover assay. The analysis of *OsIAA* protein degradation *in vitro* was performed as described⁵⁶ with minor modifications. In brief, total protein extracts were prepared from 9-day-old rice seedlings grown in MS/sucrose medium using ice-cold extraction buffer (50 mM Tris-HCl, pH 7.5, 150 mM NaCl, 0.01% Triton X-100 and 1 mM phenylmethanesulfonyl fluoride). The resulting homogenates were centrifuged at 14,000g for 15 min at 4 °C. The crude extracts (1 mg proteins) were mixed with 2 μg of purified His-OsIAA11 or His-OsIAA13 recombinant proteins in a total volume of 1 ml containing 50 μM MG132 or an equal volume DMSO as a control. The mixture was incubated at 4 °C with gentle agitation and 20 μl of each sample was collected at the indicated time points and then analysed by immunoblotting.

Co-immunoprecipitation experiments. The Co-IP experiments were performed according to the previously described methods with minor modifications⁵⁷. To prepare total cellular proteins, plant samples were ground in liquid nitrogen, and then extracted in grinding buffer (50 mM Tris-HCl, pH 7.5, 150 mM NaCl, 10 mM MgCl₂, 10% glycerol, 0.1% Nonidet P-40, 1 mM phenylmethylsulfonyl fluoride and 10 mM MG132). The extracts were cleared by centrifugation at 14,000g for 15 min at 4 °C.

For the Co-IP experiments using rice protein samples, the extracts containing 1–2 mg of proteins were incubated with 10 μl of the anti-*OsIAA11* or anti-*OsIAA13* antibodies for 1 h at 4 °C with gentle shaking. Protein A-agarose beads (100 μl; Sigma-Aldrich) were added and incubated for an additional 2–3 h at 4 °C. The immunoprecipitates were washed six times with 1 ml washing buffer (grinding buffer without MG132) and then used for immunoblotting.

For the Co-IP experiments using samples prepared from *Agrobacterium*-infiltrated *N. benthamiana* leaves, the extracts containing 1–2 mg of total proteins were incubated with 10 μl of protein A-agarose (Sigma-Aldrich) for 1 h at 4 °C, followed by adding 100 μl of anti-DDDDK-tag pAb-Agarose beads (MBL

International) and incubating for an additional 2–3 h at 4 °C. The pellets were washed six times with 1 ml washing buffer and then used for immunoblotting.

To analyse the OsTIR1 receptor complex^{15,38}, the OsTIR1-Myc fusion protein was transiently expressed in tobacco leaves by the *Agrobacterium*-mediated transformation and purified by immunoprecipitation using an anti-cMyc antibody (EarthOx Life Science). In brief, the crude protein extracts were prepared using a slightly modified extraction buffer (50 mM Tris-HCl, pH 7.5, 150 mM NaCl, 10 mM MgCl₂, 10% glycerol, 0.1% Nonidet P-40, 1 mM PMSF and 10 μM MG132) from tobacco leaves infiltrated with *Agrobacterium* cells containing a 35S:OsTIR1-Myc expression vector, and the extracts were cleared by centrifugation at 14,000g for 15 min. The protein extracts (1–2 mg of total proteins) were incubated with 5 μl of anti-cMyc antibodies for 1 h at 4 °C, and then 100 μl of protein A-agarose (Sigma-Aldrich) was added and incubated for an additional 2–3 h at 4 °C. After washing six times, the beads were mixed with protein extracts prepared from wild-type (Nipponbare) or *lrt2* seedlings (1–2 mg of proteins), 2 μg of purified His-OsIAA11 or His-OsIAA13 recombinant proteins and IAA at the indicated concentrations. The reaction was run at 4 °C for 2–3 h with gentle shaking, and the beads were washed six times and subsequently used for immunoblotting.

NMR analysis. The NMR analysis was performed according to the previously described methods with minor modifications²⁶. All NMR experiments were performed on an Agilent 600 MHz NMR spectrometer equipped with a cold probe at 25 °C. The lyophilized peptide powder (GL Biochem) was dissolved in 20 mM phosphate buffer (pH 6.5) with or without 0.05 mM LRT2 recombinant proteins, and the final concentration of the peptide was 2 mM. For all the ROESY experiments, 1,024 × 256 complex points were collected with the spectra widths of 7668.7 Hz in both dimensions. For each sample of LRT2 protein, a series of ROESY experiments were run with mixing time of 30, 50, 70, 90, 110 and 130 ms. For the control samples (samples without LRT2 protein), the longest mixing time in the series was used to carry out the ROESY experiment for comparison. All ROESY spectra were collected using 16 scans per fid with spinlock field strength of 2.8 KHz and 1 s delay time. For the assigning of the signals, TOCSY spectra were collected using 80 ms mixing time and 8 scans per fid with a spinlock field strength of 7 KHz. Signals of the *trans* and *cis* conformers were distinguished using the NOEs between the proline residue and its preceding residue⁵⁸. The ratios of cross to diagonal peak intensities for *cis* and *trans* conformations in the ROESY spectra were dependent on the total exchange rate constant k_{ex} of a two-state exchange process (*cis* ↔ *trans*) and the mixing time of the ROESY experiments (t_m). The exchange rate constants were obtained by fitting one of the following equations using different ratios with different mixing times^{59,60}.

$$I_{ct}/I_{cc} = a \cdot k_{ex} \cdot [\exp(k_{ex}t_m) - 1] / [b \cdot k_{ex} \cdot \exp(k_{ex}t_m) + a \cdot k_{ex}] \quad (1)$$

$$I_{ct}/I_{tt} = b \cdot k_{ex} \cdot [\exp(k_{ex}t_m) - 1] / [a \cdot k_{ex} \cdot \exp(k_{ex}t_m) + b \cdot k_{ex}] \quad (2)$$

where I_{cc} and I_{tt} are the diagonal peak intensities for the *cis* and *trans* conformers, and I_{ct} and I_{tc} are the cross peak intensities for the *cis*-to-*trans* and *trans*-to-*cis* exchange. a and b were determined from the normalized integration of separated peaks from *cis* and *trans* conformer of a 1D ¹H spectrum and the catalysed forward (k_{ct}^{cat}) and backward (k_{tc}^{cat}) rates equal to $a \cdot k_{ex}$ and $b \cdot k_{ex}$ respectively. The total exchange rate constant $k_{ex} = k_{ct}^{cat} + k_{tc}^{cat}$.

Structure modelling. Modelling of the 3D structure of LRT2 was performed as previously described⁵⁴ through the SWISS-Model server (<http://swissmodel.expasy.org>) using the crystal structure of wheat TaCypA-1 (PDB ID: 4E1Q) as a template⁵⁴. Molecular graphics were presented using PyMOL software (<http://www.pymol.org/>).

References

- Dharmasiri, N. & Estelle, M. Auxin signaling and regulated protein degradation. *Trends Plant Sci.* **9**, 302–308 (2004).
- Peer, W. A. From perception to attenuation: auxin signalling and responses. *Curr. Opin. Plant Biol.* **16**, 561–568 (2013).
- Wang, R. & Estelle, M. Diversity and specificity: auxin perception and signaling through the TIR1/AFB pathway. *Curr. Opin. Plant Biol.* **21**, 51–58 (2014).
- Kepinski, S. & Leyser, O. The *Arabidopsis* F-box protein TIR1 is an auxin receptor. *Nature* **435**, 446–451 (2005).
- Dharmasiri, N., Dharmasiri, S. & Estelle, M. The F-box protein TIR1 is an auxin receptor. *Nature* **435**, 441–445 (2005).
- Tan, X. *et al.* Mechanism of auxin perception by the TIR1 ubiquitin ligase. *Nature* **446**, 640–645 (2007).
- Gray, W. M., Kepinski, S., Rouse, D., Leyser, O. & Estelle, M. Auxin regulates SCF^{TIR1}-dependent degradation of AUX/IAA proteins. *Nature* **414**, 271–276 (2001).
- Tiwari, S. B., Wang, X.-J., Hagen, G. & Guilfoyle, T. J. AUX/IAA proteins are active repressors, and their stability and activity are modulated by auxin. *Plant Cell* **13**, 2809–2822 (2001).
- Liscum, E. & Reed, J. W. Genetics of Aux/IAA and ARF action in plant growth and development. *Plant Mol. Biol.* **49**, 387–400 (2002).
- Reed, J. W. Roles and activities of Aux/IAA proteins in *Arabidopsis*. *Trends Plant Sci.* **6**, 420–425 (2001).
- Mockaitis, K. & Estelle, M. Auxin receptors and plant development: a new signaling paradigm. *Annu. Rev. Cell Dev. Biol.* **24**, 55–80 (2008).
- Ramos, J. A., Zenser, N., Leyser, O. & Callis, J. Rapid degradation of auxin/indoleacetic acid proteins requires conserved amino acids of domain II and is proteasome dependent. *Plant Cell* **13**, 2349–2360 (2001).
- Tian, Q., Nagpal, P. & Reed, J. W. Regulation of *Arabidopsis* SHY2/IAA3 protein turnover. *Plant J.* **36**, 643–651 (2003).
- Yang, X. *et al.* The IAA1 protein is encoded by *AXR5* and is a substrate of SCF^{TIR1}. *Plant J.* **40**, 772–782 (2004).
- Dharmasiri, N., Dharmasiri, S., Jones, A. M. & Estelle, M. Auxin action in a cell-free system. *Curr. Biol.* **13**, 1418–1422 (2003).
- Zheng, H. *et al.* LATERAL ROOTLESS2, a cyclophilin protein, regulates lateral root initiation and auxin signaling pathway in rice. *Mol. Plant* **6**, 1719–1721 (2013).
- Kang, B. *et al.* OsCYP2, a chaperone involved in degradation of auxin-responsive proteins, plays crucial roles in rice lateral root initiation. *Plant J.* **74**, 86–97 (2013).
- Romano, P. G. N., Horton, P. & Gray, J. E. The *Arabidopsis* cyclophilin gene family. *Plant Physiol.* **134**, 1268–1282 (2004).
- Lu, K. P., Finn, G., Lee, T. H. & Nicholson, L. K. Prolyl *cis-trans* isomerization as a molecular timer. *Nat. Chem. Biol.* **3**, 619–629 (2007).
- Gasser, C. S., Gunning, D. A., Budelier, K. A. & Brown, S. M. Structure and expression of cytosolic cyclophilin/peptidyl-prolyl *cis-trans* isomerase of higher plants and production of active tomato cyclophilin in *Escherichia coli*. *Proc. Natl. Acad. Sci. USA* **87**, 9519–9523 (1990).
- Kumari, S., Roy, S., Singh, P., Singla-Pareek, S. & Pareek, A. Cyclophilins: proteins in search of function. *Plant Signal Behav.* **8**, e22734 (2013).
- Vasudevan, D. *et al.* Plant immunophilins: a review of their structure-function relationship. *Biochim. Biophys. Acta* doi:10.1016/j.bbagen.2014.12.017 (19 December 2014).
- Trupkin, S. A., Mora-García, S. & Casal, J. J. The cyclophilin ROC1 links phytochrome and cryptochrome to brassinosteroid sensitivity. *Plant J.* **71**, 712–723 (2012).
- Ma, X., Song, L., Yang, Y. & Liu, D. A gain-of-function mutation in the ROC1 gene alters plant architecture in *Arabidopsis*. *New Phytol.* **197**, 751–762 (2013).
- Zhang, Y. *et al.* The cyclophilin CYP20-2 modulates the conformation of BRASSINAZOLE-RESISTANT1, which binds the promoter of FLOWERING LOCUS D to regulate flowering in *Arabidopsis*. *Plant Cell* **25**, 2504–2521 (2013).
- Wang, Y., Liu, C., Yang, D., Yu, H. & Liou, Y.-C. *Pin1At* encoding a peptidyl-prolyl *cis/trans* isomerase regulates flowering time in *Arabidopsis*. *Mol. Cell* **37**, 112–122 (2010).
- Li, M. *et al.* Proline isomerization of the immune receptor-interacting protein RIN4 by a cyclophilin inhibits effector-triggered immunity in *Arabidopsis*. *Cell Host Microbe* **16**, 473–483 (2014).
- Oh, K., Ivanchenko, M., White, T. J. & Lomax, T. The *diageotropica* gene of tomato encodes a cyclophilin: a novel player in auxin signaling. *Planta* **224**, 133–144 (2006).
- Ivanchenko, M. G., Coffeen, W. C., Lomax, T. L. & Dubrovsky, J. G. Mutations in the *Diageotropica* (*Dgt*) gene uncouple patterned cell division during lateral root initiation from proliferative cell division in the pericycle. *Plant J.* **46**, 436–447 (2006).
- Lavy, M., Prigge, M. J., Tigyi, K. & Estelle, M. The cyclophilin DIAGEOTROPICA has a conserved role in auxin signaling. *Development* **139**, 1115–1124 (2012).
- Zhu, Z.-X. *et al.* A gain-of-function mutation in *OsIAA11* affects lateral root development in rice. *Mol. Plant* **5**, 154–161 (2012).
- Kitomi, Y., Inahashi, H., Takehisa, H., Sato, Y. & Inukai, Y. OsIAA13-mediated auxin signaling is involved in lateral root initiation in rice. *Plant Sci.* **190**, 116–122 (2012).
- Jun, N. *et al.* OsIAA23-mediated auxin signaling defines postembryonic maintenance of QC in rice. *Plant J.* **68**, 433–442 (2011).
- Sekhon, S. S. *et al.* Structural and biochemical characterization of the cytosolic wheat cyclophilin TaCypA-1. *Acta Crystallogr. D Biol. Crystallogr.* **69**, 555–563 (2013).
- Reimer, U. *et al.* Side-chain effects on peptidyl-prolyl *cis/trans* isomerisation. *J. Mol. Biol.* **279**, 449–460 (1998).
- Schönbrunner, E. R. *et al.* Catalysis of protein folding by cyclophilins from different species. *J. Biol. Chem.* **266**, 3630–3635 (1991).
- Endrich, M. M., Gehrig, P. & Gehring, H. Maturation-induced conformational changes of HIV-1 capsid protein and identification of two high affinity sites for cyclophilins in the C-terminal domain. *J. Biol. Chem.* **274**, 5326–5332 (1999).
- Kepinski, S. & Leyser, O. Auxin-induced SCF^{TIR1}-Aux/IAA interaction involves stable modification of the SCF^{TIR1} complex. *Proc. Natl. Acad. Sci. USA* **101**, 12381–12386 (2004).

39. Gray, W. M., Muskett, P. R., Chuang, H.-W. & Parker, J. E. *Arabidopsis* SGT1b is required for SCF^{TIR1}-mediated auxin response. *Plant Cell* **15**, 1310–1319 (2003).
40. Zhao, Y., Dai, X., Blackwell, H. E., Schreiber, S. L. & Chory, J. SIR1, an upstream component in auxin signaling identified by chemical genetics. *Science* **301**, 1107–1110 (2003).
41. Pérez-Pérez, J. M., Ponce, M. R. & Micol, J. L. The *ULTRACURVATA2* gene of *Arabidopsis* encodes an FK506-binding protein involved in auxin and brassinosteroid signaling. *Plant Physiol.* **134**, 101–117 (2004).
42. Li, B. *et al.* Integrative study on proteomics, molecular physiology, and genetics reveals an accumulation of cyclophilin-like protein, TaCYP20-2, leading to an increase of Rht protein and dwarf in a novel GA-insensitive mutant (*gaid*) in wheat. *J. Proteome Res.* **9**, 4242–4253 (2010).
43. Park, S.-W. *et al.* Cyclophilin 20-3 relays a 12-oxo-phytyldienoic acid signal during stress responsive regulation of cellular redox homeostasis. *Proc. Natl. Acad. Sci. USA* **110**, 9559–9564 (2013).
44. Hirano, K., Ueguchi-Tanaka, M. & Matsuoka, M. *GID1*-mediated gibberellin signaling in plants. *Trends Plant Sci.* **13**, 192–199 (2008).
45. Sun, T.-p. The molecular mechanism and evolution of the GA-*GID1*-*DELLA* signaling module in plants. *Curr. Biol.* **21**, R338–R345 (2011).
46. Pérez, A. C. & Goossens, A. Jasmonate signalling: a copycat of auxin signalling? *Plant Cell Environ.* **36**, 2071–2084 (2013).
47. Jiang, L. *et al.* *DWARF 53* acts as a repressor of strigolactone signalling in rice. *Nature* **504**, 401–405 (2013).
48. Zhou, F. *et al.* *D14-SCF^{D3}* dependent degradation of *D53* regulates strigolactone signalling. *Nature* **504**, 406–410 (2013).
49. Wang, H., Taketa, S., Miyao, A., Hirochika, H. & Ichii, M. Isolation of a novel lateral-rootless mutant in rice (*Oryza sativa* L.) with reduced sensitivity to auxin. *Plant Sci.* **170**, 70–77 (2006).
50. Hiei, Y., Ohta, S., Komari, T. & Kumashiro, T. Efficient transformation of rice (*Oryza sativa* L.) mediated by *Agrobacterium* and sequence analysis of the boundaries of the T-DNA. *Plant J.* **6**, 271–282 (1994).
51. Chen, H. *et al.* Firefly luciferase complementation imaging assay for protein-protein interactions in plants. *Plant Physiol.* **146**, 368–376 (2008).
52. Wang, Z. *et al.* A practical vector for efficient knockdown of gene expression in rice (*Oryza sativa* L.). *Plant Mol. Biol. Rep.* **22**, 409–417 (2004).
53. Ding, Y.-H., Liu, N.-Y., Tang, Z.-S., Liu, J. & Yang, W.-C. *Arabidopsis GLUTAMINE-RICH PROTEIN23* is essential for early embryogenesis and encodes a novel nuclear PPR motif protein that interacts with RNA polymerase II subunit III. *Plant Cell* **18**, 815–830 (2006).
54. Feng, J. *et al.* S-nitrosylation of phosphotransfer proteins represses cytokinin signaling. *Nat. Commun.* **4**, 1529 (2013).
55. Liu, H. *et al.* Photoexcited *CRY2* interacts with *CIB1* to regulate transcription and floral initiation in *Arabidopsis*. *Science* **322**, 1535–1539 (2008).
56. Nakamura, A. *et al.* Production and characterization of auxin-insensitive rice by overexpression of a mutagenized rice IAA protein. *Plant J.* **46**, 297–306 (2006).
57. Dharmasiri, N. *et al.* Plant development is regulated by a family of auxin receptor F box proteins. *Dev. Cell* **9**, 109–119 (2005).
58. Ramelot, T. A. & Nicholson, L. K. Phosphorylation-induced structural changes in the amyloid precursor protein cytoplasmic tail detected by NMR. *J. Mol. Biol.* **307**, 871–884 (2001).
59. Pastorino, L. *et al.* The prolyl isomerase *Pin1* regulates amyloid precursor protein processing and amyloid- β production. *Nature* **440**, 528–534 (2006).
60. Pastorino, L. *et al.* The prolyl isomerase *Pin1* regulates amyloid precursor protein processing and amyloid- β production. *Nature* **446**, 342–342 (2007).

Acknowledgements

We thank Dr Xiaorong Mo for *cyp2-2* mutant seeds; Dr Ping Wu for *osiaa11* mutant seeds; Dr Yoshiaki Inukai for *osiaa13* seeds; Drs Kang Chong, Jian-Min Zhou and Wei-Cai Yang for expression vectors; Dr Kang Chong for sharing the unpublished data; Drs Makoto Matsuoka and Yuling Jiao for critical reading the manuscript and valuable comments; Dr Neing Yan and members of Zuo laboratory for helpful discussion. This work was supported by grants from the National Natural Science Foundation of China (91217302), the Ministry of Science and Technology of China (2014CB943402) and State Key Laboratory of Plant Genomics (Y260022512).

Author contributions

H.J., X.Y., X.L., Q.Q., J.L. and J.Zuo. designed the experiments. H.J. and X.Y. performed the majority of the experiments, assisted by J.Zhang, X.L., H.Z., G.D., J.N. and J.F. All authors analysed the data and commented on the manuscript. H.J., X.Y., X.L., B.X., J.L. and J.Zuo. wrote the manuscript.

Additional information

Supplementary Information accompanies this paper at <http://www.nature.com/naturecommunications>

Competing financial interests: The authors declare no competing financial interests.

Reprints and permission information is available online at <http://npg.nature.com/reprintsandpermissions/>

How to cite this article: Jing, H. *et al.* Peptidyl-prolyl isomerization targets rice Aux/IAAs for proteasomal degradation during auxin signalling. *Nat. Commun.* 6:7395 doi: 10.1038/ncomms8395 (2015).